DALTON

Photoluminescence, photoredox properties and crystal structures of rhenium(v)–benzylidyne complexes with phosphine ligands †

Wen-Mei Xue,[a] Yue Wang,[a] Thomas C. W. Mak[b] and Chi-Ming Che*[,a]

[a] *Department of Chemistry, The University of Hong Kong, Pokfulam Road, Hong Kong*
[b] *Department of Chemistry, The Chinese University of Hong Kong, Shatin, New Territories, Hong Kong*

Several rhenium(v)–benzylidyne complexes $[Re(CR)(pdpp)_2Cl]^+$ [R = $C_6H_2Me_3$-2,4,6, pdpp = *o*-phenylenebis(diphenylphosphine)], $[Re(CR)L_2(CO)(H_2O)Cl]^+$ [L = PPh_3, $P(C_6H_4OMe\text{-}p)_3$ or PMe_2Ph] and *trans*-$[Re(CR)(dppe)(CO)_2Cl]^+$ [dppe = 1,2-bis(diphenylphosphino)ethane] have been prepared. The structures of *trans*-$[Re(CR)(pdpp)_2Cl]ClO_4 \cdot CHCl_3 \cdot 0.25MeOH$ and $[Re(CR)(PPh_3)_2(CO)(H_2O)Cl]ClO_4 \cdot 1.5MeOH$ have been determined by X-ray analyses. The Re≡C distances are 1.802(5) and 1.784(8) Å respectively. In acetonitrile and dichloromethane the complexes show intense absorption bands at 318–330 nm and weak ones at 405–450 nm, the latter being tentatively assigned to $d_{xy} \longrightarrow d_{\pi^*}$ (d_{xz},d_{yz}) transitions. Photoexcitation in the solution, solid or glassy state gives intense orange to red emissions, and the emitting states are tentatively assigned to $^3[(d_{xy})^1(d_{\pi^*})^1]$. The variation in non-radiative decay rate constants for the emissions of the rhenium(v)–benzylidyne complexes are consistent with a prediction from the energy-gap law. The excited states are better oxidants and reductants than the ground states. The values of $E°(Re^{V*}\text{–}Re^{IV})$ and $E°(Re^{VI}\text{–}Re^{V*})$ in acetonitrile have been determined using spectroscopic and electrochemical data as well as by Stern–Volmer quenching experiments.

The design of photoluminescent metal complexes with long-lived excited states for photoinduced electron-transfer reactions has been an area of considerable interest. Recent studies have revealed the intriguing photo-physical and -chemical properties of d^2-metal complexes in which the metal atom is multiply bonded to a heteroatom, such as oxygen and nitrogen.[1–4] In some of these complexes the $^3[(d_{xy})^1(d_{\pi^*})^1]$ excited states have been found to be long lived and emissive in solution at room temperature. It was anticipated that population of an electron in the d_{π^*} orbital would weaken the metal–ligand multiple bond. Thus these complexes, if suitably designed, are potent reagents for photoinduced atom-transfer reactions.

Previously, Mayr and others[5] reported that d^2 tungsten(IV)–alkylidyne complexes are luminescent. However, these tungsten complexes have emission lifetimes hardly greater than 1 μs in solution at room temperature, rendering difficult some of the Stern–Volmer kinetic experiments. The rich photoluminescence and photochemical properties displayed by *trans*-dioxo- and nitrido-rhenium(v) complexes[4] led us to investigate the photo-physical and -chemical properties of the isoelectronic rhenium(v) benzylidyne complexes, with an objective to develop highly reactive metal–benzylidyne complexes through light excitation. Rhenium(v)–alkylidyne and –benzylidyne complexes have been reported,[6] but their photochemical properties have not been noted. Herein we describe the spectroscopic and photoredox properties of several rhenium(v)–benzylidyne complexes containing phosphine ligands.

Experimental

All manipulations were carried out under a nitrogen atmosphere using standard Schlenk techniques. Solvents were distilled over sodium–benzophenone (tetrahydrofuran and toluene), CaH_2 (dichloromethane) and $Na_{2.8}K$ alloy (light petroleum, b.p. 40–60 °C). Dichloromethane for photophysical studies was washed with concentrated sulfuric acid, 10% sodium hydrogencarbonate and water, then dried by calcium chloride and distilled over calcium hydride. Acetonitrile was distilled over potassium permanganate and then calcium hydride. The other solvents used were of analytical grade. The compounds $[Re_2(CO)_{10}]$ (Strem), 2,4,6-trimethylbenzoyl chloride (Lancaster), trifluoromethanesulfonic anhydride, $(CF_3SO_2)_2O$ (Aldrich), *o*-phenylenebis(diphenylphosphine) (pdpp, Strem), triphenylphosphine (Merck), tris(*p*-methoxyphenyl)phosphine (Strem), methyldiphenylphosphine (Strem) and 1,2-bis(diphenylphosphino)ethane (dppe, Aldrich) were used as received; $[Re\{C(O)C_6H_2Me_3\text{-}2,4,6\}(CO)_5]$ was prepared by the literature method.[6d] The pyridinium salts for quenching studies were prepared by refluxing the corresponding pyridines with methyl iodide in acetone–ethanol (1:1, v/v) for 4 h, followed by metathesis in water using potassium hexafluorophosphate and recrystallization from acetonitrile–diethyl ether. Amine quenchers were purified according to literature procedures.[7]

Preparations

***trans*-$[Re(CC_6H_2Me_3\text{-}2,4,6)(CO)_4Cl][O_3SCF_3]$ 1.** The compound $[Re\{C(O)C_6H_2Me_3\text{-}2,4,6\}(CO)_5]$ (1.68 g, 3.56 mmol) was dissolved in dichloromethane (30 cm^3) and the solution chilled to −40 °C in an acetone–solid CO_2 bath. Trifluoromethanesulfonic anhydride (0.60 cm^3, 3.56 mmol) in dichloromethane (10 cm^3) was added dropwise while stirring rapidly. After stirring at −40 °C for 30 min the solvent was removed, and the residue washed with toluene (2 × 5 cm^3) and light petroleum (4 × 15 cm^3) to afford the yellow product **1** (yield ≈95%). Mass spectrum (positive FAB): *m*/*z* 465 (M^+), 437 (M^+ − CO), 409 (M^+ − 2CO) and 355 (M^+ − 4CO). IR: ν̃(C≡O) 2144m, 2117m, 2094m and 1993m cm^{-1}.

***trans*-$[Re(CC_6H_2Me_3\text{-}2,4,6)(pdpp)_2Cl]ClO_4$ 2.** A mixture of complex **1** (0.40 g, 0.65 mmol) and pdpp (0.58 g, 1.30 mmol) in tetrahydrofuran (40 cm^3) was refluxed for 12 h. A bright yellow solution was obtained. The solvent was removed *in vacuo* and the yellow solid dissolved in methanol (10 cm^3). The product

† *Non-SI unit employed:* eV ≈ 1.60 × 10^{-19} J.

was precipitated with $LiClO_4$ (0.50 g) and then recrystallized by diffusion of diethyl ether into a chloroform solution containing a small amount of methanol (yield ≈50%) (Found: C, 56.20; H, 4.40. Calc. for $C_{70}H_{59}Cl_2O_4P_4Re\cdot1.5CHCl_3\cdot0.25CH_3OH$: C, 56.25; H, 4.00%). Mass spectrum (positive FAB); *m/z* 1246 (M^+) and 799 (M^+ − pdpp). NMR (CD_2Cl_2): ^1H, δ 7.72–6.27 (50, aryl H), 2.06 (s, 3, *p*-Me) and 1.58 (s, 6, *o*-Me); ^{13}C, δ 268.8 (Re≡C), 145.2–127.6 (aryl C), 21.6 (*p*-Me) and 21.1 (*o*-Me); ^{31}P, δ 31.3.

[Re(CC$_6$H$_2$Me$_3$-2,4,6)(PPh$_3$)$_2$(CO)(H$_2$O)Cl]ClO$_4$ 3. A mixture of complex **1** (0.40 g, 0.65 mmol) and PPh_3 (0.68 g, 2.6 mmol) in tetrahydrofuran (40 cm^3) was refluxed for 16 h. A bright yellow solution was obtained. The solvent was removed *in vacuo* and methanol (10 cm^3) added to dissolve the complex. The unreacted PPh_3 was filtered off. Lithium perchlorate (0.50 g) was added to the filtrate followed by diethyl ether (30 cm^3). Yellow crystals of the complex gradually deposited (yield ≈30%). Mass spectrum (positive FAB): *m/z* 905 ($M^+ - H_2O$) and 643 ($M^+ - H_2O - PPh_3$). IR: ν̃(C≡O) 1988s cm^{-1}. NMR ($CDCl_3$): ^1H, δ 7.70–6.60 (32, aryl H), 2.21 (s, 3, *p*-Me) and 1.70 (s, 6, *o*-Me); ^{13}C, δ 204.0 (CO), 143.3–128.5 (aryl C), 21.9 (*p*-Me) and 19.3 (*o*-Me); ^{31}P, δ 14.4.

[Re(CC$_6$H$_2$Me$_3$-2,4,6){P(C$_6$H$_4$OMe-*p*)$_3$}$_2$(CO)(H$_2$O)Cl][O$_3$SCF$_3$] 4. A mixture of complex **1** (0.40 g, 0.65 mmol) and $P(C_6H_4OMe\text{-}p)_3$ (0.92 g, 2.6 mmol) in tetrahydrofuran (40 cm^3) was refluxed for 12 h to give a bright yellow solution. The solvent was removed *in vacuo* and methanol (10 cm^3) added to dissolve the complex. The unreacted phosphine was filtered off and the filtrate evaporated to dryness to give the crude product, which was chromatographed on a silica gel (230–400 mesh) column with light petroleum–diethyl ether (1 : 1 v/v) and then diethyl ether–dichloromethane (5 : 1 v/v) as eluent. The solvent mixture was removed *in vacuo* and the yellow solid recrystallized from ethanol–dichloromethane (5 : 1 v/v) to give yellow crystals (yield ≈20%) (Found: C, 56.50; H, 4.60. Calc. for $C_{54}H_{55}ClF_3O_{11}P_2ReS\cdot6C_4H_4O$: C, 56.40; H, 4.75%). Mass spectrum (positive FAB): *m/z* 1085 ($M^+ - H_2O$) and 733 [$M^+ - H_2O - P(C_6H_4OMe\text{-}p)_3$]. IR: ν̃(C≡O) 1978m cm^{-1}. NMR ($CDCl_3$): ^1H, δ 7.65–6.44 (26, aryl H), 3.75 (s, 18, OMe), 2.14 (s, 3, *p*-Me) and 1.75 (s, 6, *o*-Me); ^{13}C, δ 277.0 (Re≡C), 206.1 (CO), 160.6–113.1 (aryl C), 55.1 (OMe) and 21.7 (Me).

[Re(CC$_6$H$_2$Me$_3$-2,4,6)(PMePh$_2$)$_2$(CO)(H$_2$O)Cl]ClO$_4$ 5. A mixture of complex **1** (0.40 g, 0.65 mmol) and $PMePh_2$ (0.40 cm^3, 2.1 mmol) in tetrahydrofuran (40 cm^3) was refluxed for 12 h to give a bright yellow solution. This was evaporated to dryness under vacuum. The unreacted $PMePh_2$ was removed by washing the subsequent product mixture with light petroleum. A yellow oil was obtained which was dissolved in methanol (10 cm^3). Upon addition of $LiClO_4$ (0.50 g) and cooling to −80 °C yellow crystals of the product formed (yield ≈20%) {Found: C, 53.90; H, 4.40. Calc. for [Re(C$_{10}$H$_{11}$)(C$_{13}$H$_{13}$P)$_2$(CO)(H$_2$O)Cl]ClO$_4$·3C$_4$H$_4$O: C, 53.35; H, 4.65%. Mass spectrum (positive FAB): *m/z* 781 ($M^+ - H_2O$), 753 ($M^+ - CO - H_2O$) and 581 ($M^+ - PMePh_2 - H_2O$). IR: ν̃(C≡O) 1984s cm^{-1}. NMR ($CDCl_3$): ^1H, δ 7.86–6.46 (22, aryl H), 2.34 (s, 6, *o*-Me), 2.14 (s, 3, *p*-Me) and 1.59 (s, 6, PMe); ^{13}C, δ 278.3 (Re≡C), 205.9 (CO), 141.7–127.5 (aryl C), 21.8 (Me) and 12.8 (PMe).

***trans*-[Re(CC$_6$H$_2$Me$_3$-2,4,6)(dppe)(CO)$_2$Cl]ClO$_4$ 6.** A mixture of complex **1** (0.20 g, 0.32 mmol) and dppe (0.25 g, 0.64 mmol) in tetrahydrofuran (20 cm^3) was refluxed for 6 h to give a bright yellow solution. This was evaporated to dryness *in vacuo* and the solid residue dissolved in methanol (5 cm^3). Upon addition of $LiClO_4$ (0.30 g) a yellow solid precipitated. This was purified on a silica gel (230–400 mesh) column packed with diethyl ether using chloroform as eluent (yield ≈70%) (Found: C, 53.35; H, 4.55; Cl, 6.25. Calc. for $C_{38}H_{35}Cl_2O_6P_2Re\cdot2C_4H_4O$: C, 52.95; H, 4.15; Cl, 6.80%). Mass spectrum (positive FAB): *m/z* 807 (M^+) and 751 (M^+ − 2CO). IR: ν̃(C≡O) 2006m and 1968m cm^{-1}. NMR ($CDCl_3$): δ 7.82–6.99 (22, aryl H), 2.26–2.10 (4, CH_2), 1.84 (s, 6, *o*-Me) and 1.64 (s, 3, *p*-Me); ^{13}C, δ 279.1 (Re≡C), 198.3 (CO), 188.9 (CO), 144.2–126.9 (aryl C), 26.5 (CH_2), 21.9 (*p*-Me) and 18.5 (*o*-Me).

Crystallography

Crystals of *trans*-[Re(CC$_6$H$_2$Me$_3$-2,4,6)(pdpp)$_2$Cl]ClO$_4$·CHCl$_3$·0.25MeOH were obtained by diffusion of diethyl ether into a chloroform–methanol (10 : 1) solution. A pale yellow prism crystal with dimensions 0.20 × 0.20 × 0.60 mm was used for X-ray analysis. Intensity data were collected on a Rigaku RAXIS-IIC imaging-plate system using Mo-Kα radiation (λ = 0.710 73 Å) from a Ru-200 rotating-anode X-ray generator operating at 50 kV and 90 mA at room temperature. The data were corrected for absorption and Lorentz-polarization effects. The structure was solved by Patterson and Fourier methods and subsequently refined on *F* by full-matrix least squares using the SHELXTL-PC package.[8] The last least-squares cycle was calculated with 785 parameters, *p*, and 9220 reflections, *n*, [$|F_o| > 10\sigma(|F_o|)$] out of 12 080 unique data measured. The final Fourier-difference map showed residual extrema in the range of +0.95 to −1.40 e $Å^{-3}$. The perchlorate ion has two equally populated orientations, and the chloroform solvent molecule exhibits two-fold disorder about one of the C–Cl bonds. The residual electron density which persists in a void in the crystal can be modelled by atom C(72) with half-site occupation, which is approximately equivalent to ¼ of a methanol molecule in regard to scattering power. The crystallographic data are summarized in Table 1. Selected bond distances and angles are listed in Table 2.

Crystals of [Re(CC$_6$H$_2$Me$_3$-2,4,6)(PPh$_3$)$_2$(CO)(H$_2$O)Cl]ClO$_4$·1.5MeOH were obtained by slow diffusion of diethyl ether into methanol solution of the complex. A golden needle crystal with dimensions 0.08 × 0.10 × 0.20 mm was used for X-ray analysis. The last least-squares cycle was calculated with 466 parameters, *p*, and 7486 reflections, *n*, [$|F_o| > 3\sigma(|F_o|)$] out of 8524 unique data measured. The final Fourier-difference map showed residual extrema in the range of +0.92 to −0.68 e $Å^{-3}$. In each complex the H atoms were generated geometrically knowing the hybridisation state of the parent C atom. In the case of a CH_3 group attached to a planar aromatic ring (*e.g.* phenyl or pyridyl), its approximate orientation was established provided at least one H atom could be located from a difference map. The CH_3 group was then treated as a rigid group. All H atoms were assigned fixed isotropic thermal parameters and allowed to ride on their respective parent C atoms. Selected bond distances and angles are listed in Table 3.

Atomic coordinates, thermal parameters and bond lengths and angles have been deposited at the Cambridge Crystallographic Data Centre (CCDC). See Instructions for Authors, *J. Chem. Soc., Dalton Trans.*, 1996, Issue 1. Any request to the CCDC for this material should quote the full literature citation and the reference number 186/74.

Physical measurements

Infrared spectra were recorded on a Nicolet 20FXC FT-IR spectrophotometer, UV/VIS absorption spectra on a Milton Roy Spectronic 3000 diode-array spectrophotometer, ^1H, ^{13}C and ^{31}P NMR spectra on a JEOL 270 MHz Fourier-transform spectrometer with $SiMe_4$ (^1H and ^{13}C) or H_3PO_4 (^{31}P) as internal reference. Elemental analyses were performed by Butterworth Laboratories (UK). Mass spectra were obtained on a Finnigan Mat 95 mass spectrometer. Cyclic voltammetry was performed with a Princeton Applied Research (PAR) model 175 universal programmer and a model 273 potentiostat coupled to a Kipp & Zoner X-Y recorder. A conventional two-

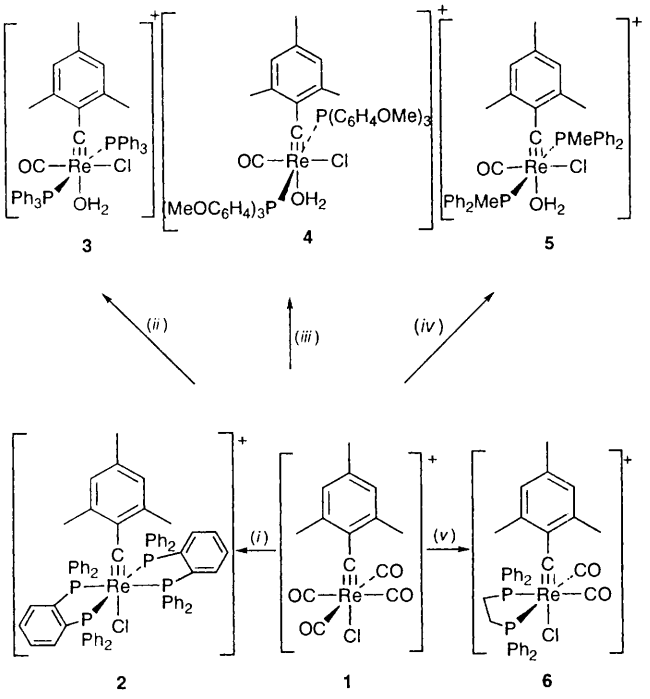

Scheme 1 (*i*) pdpp; (*ii*) PPh_3; (*iii*) $P(C_6H_4OMe\text{-}p)_3$; (*iv*) $PMePh_2$; (*v*) dppe

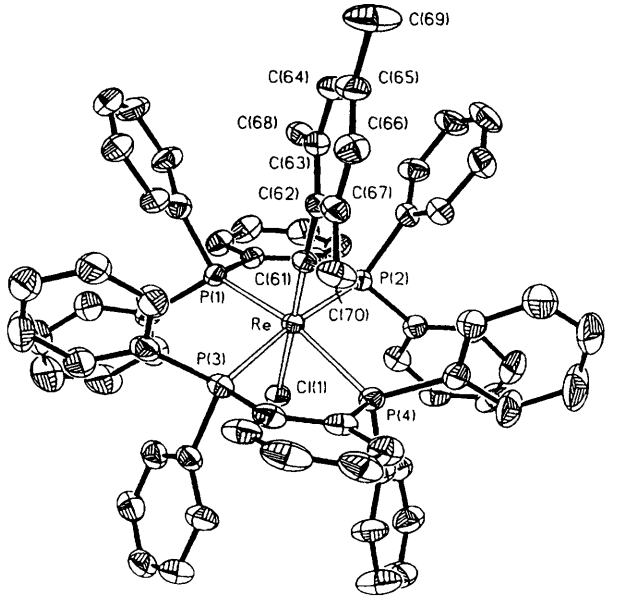

Fig. 1 A perspective view of $[Re(CC_6H_2Me_3\text{-}2,4,6)(pdpp)_2Cl]^+$

compartment cell was used with Ag–$AgNO_3$ (0.1 mol dm^{-3} in acetonitrile) as the reference electrode and ferrocenium–ferrocene as the internal standard. The supporting electrolyte was tetrabutylammonium hexafluorophosphate (0.1 mol dm^{-3}). Glassy carbon was used as the working electrode. Steady-state emission spectra were recorded on a SPEX 1681 FLUOROLOG-2 series F111AI spectrometer. The emission spectra were corrected for monochromator and photomultiplier efficiency, and for xenon-lamp stability. Emission quantum yields were determined by the literature methods.[9] Emission lifetimes were determined and flash-photolysis measurements were performed with a Quanta Ray DCR-3 pulsed Nd-YAG laser system (pulse output 355 nm, 8 ns). The emission signals were detected by a Hamamatsu R928 photomultiplier tube and recorded on a Tektronix model 2430 digital oscilloscope.

Stern–Volmer quenching experiments were carried out with degassed acetonitrile solutions of the metal complex and

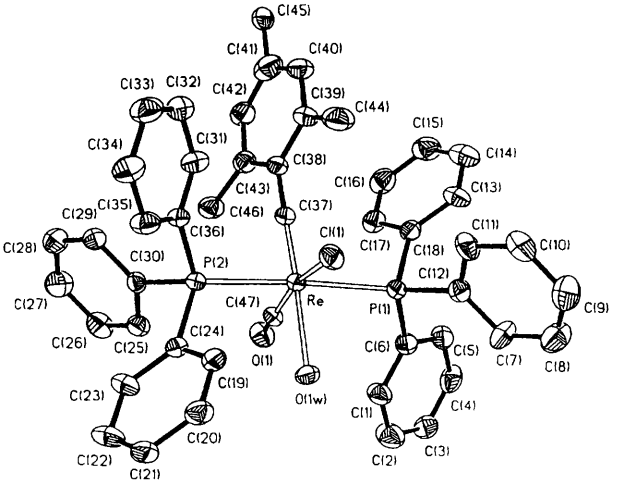

Fig. 2 A perspective view of $[Re(CC_6H_2Me_3\text{-}2,4,6)(PPh_3)_2(CO)(H_2O)Cl]^+$

quenchers (Q). In each case a linear plot of τ_0/τ *vs.* [Q] was obtained from which the quenching rate constants k_q were deduced according to the equation, $\tau_0/\tau = 1 + k_q\tau_0[Q]$, where τ_0 and τ refer to the luminescence lifetimes in the absence and presence of Q.

Results and Discussion

Syntheses

The literature methods[6a,b] for the synthesis of rhenium(v)–alkylidyne and –benzylidyne complexes containing chelating diphosphine ligands usually require many steps. In this work, *trans*-$[Re(CC_6H_2Me_3\text{-}2,4,6)(CO)_4Cl][O_3SCF_3]$ **1**, which was formed by the reaction of $[Re\{C(O)C_6H_2Me_3\text{-}2,4,6\}(CO)_5]$ with trifluoromethanesulfonic anhydride in dichloromethane, has been found to be a good starting material for rhenium(v)–benzylidyne complexes. The same reaction reported by Williams and Schrock[6d] was found to give $[Re(CC_6H_2Me_3\text{-}2,4,6)(CO)_4(O_3SCF_3)][O_3SCF_3]$ which is insoluble in common organic solvents. Complex **1**, however, is soluble in tetrahydrofuran, acetonitrile, methanol and chloroform. We speculate that the co-ordinated chloride comes from the dichloromethane. The reactions of **1** with several phosphine ligands have been studied in this work. Depending on the phosphine ligands, either two or four CO are substituted as depicted in Scheme 1. In the synthesis of **2** the displacement of four CO is probably due to the strong co-ordinating power of pdpp. For **3**, it is difficult to locate the carbyne carbon in the ^{13}C NMR spectrum, but its structure has been determined by X-ray crystallography.

Crystal structures

Figs. 1 and 2 show the respective perspective views of complexes **2** and **3**. The structures feature the first examples of rhenium(v)-2,4,6-trimethylbenzylidyne complexes. In **2** the Re–C(61) distance of 1.802(5) Å is somewhat longer than the predicted range 1.721–1.751 Å from the sum of the covalent radii of Re and sp-C atoms,[6a] but comparable to the Re≡CNHR distances in *trans*-$[ReCl(CNHR)(dppe)_2]BF_4$ [1.798(30) Å, R = Me; 1.802(4) Å, R = H],[6a,b] where there is a π-electron delocalization within the Re≡C–NHR unit. It is likely that the $Re{\equiv}CC_6H_2Me_3$ moiety in **2** behaves in a similar fashion. The Re–C(61)–C(62) angle of 175.2(5)° is close to linearity and this is not unexpected for a co-ordinated benzylidyne. The C(61)–Re–Cl(1) angle of 174.4(2)° is approximately linear and the long Re–Cl distance of 2.497(2) Å is due to the large *trans* effect of the benzylidyne ligand.

Table 1 Crystallographic data for complexes **2** and **3**

	2 *trans*-$[Re(CC_6H_2Me_3)(pdpp)_2Cl]ClO_4 \cdot CHCl_3 \cdot 0.25MeOH$	**3** $[Re(CC_6H_2Me_3)(PPh_3)_2(CO)(H_2O)Cl]ClO_4 \cdot 1.5MeOH$
Formula	$C_{71.25}H_{61}Cl_5O_{4.25}P_4Re$	$C_{48.5}H_{49}Cl_2O_{7.5}P_2Re$
M	1472.5	1071.0
a/Å	13.316(1)	11.862(2)
b/Å	14.497(1)	13.446(3)
c/Å	18.597(2)	17.252(3)
α/°	94.31(1)	100.88(3)
β/°	110.60(1)	105.35(3)
γ/°	94.58(1)	98.60(3)
U/Å^3	3325(2)	2548(1)
D_c/g cm^{-3}	1.471	1.386
μ/cm^{-1}	21.73	25.99
R	0.043	0.055
R'	0.058	0.086
S	0.94	1.72

* Details in common: triclinic, space group $P\bar{1}$ (no. 2); $Z = 2$; $R = \Sigma(|F_o| - |F_c|)/\Sigma|F_o|$; $R' = [\Sigma w(|F_o| - |F_c|)^2/\Sigma w|F_o|^2]^{\frac{1}{2}}$; $S = [\Sigma w(|F_o| - |F_c|)^2/(n - p)]^{\frac{1}{2}}$; $w = (\sigma^2|F_o| + 0.000\,002|F_o|^2)^{-1}$ for complex **2** and $(\sigma^2|F_o| + 0.001|F_o|^2)^{-1}$ for **3**.

Table 2 Selected bond distances (Å) and angles (°) for complex **2**

Re–P(1)	2.465(2)	Re–P(2)	2.460(2)
Re–P(3)	2.460(2)	Re–P(4)	2.481(2)
Re–Cl(1)	2.497(2)	Re–C(61)	1.802(5)
C(61)–C(62)	1.460(7)		
P(1)–Re–P(2)	81.0(1)	P(1)–Re–P(3)	99.3(1)
P(2)–Re–P(3)	170.4(1)	P(1)–Re–P(4)	164.7(1)
P(2)–Re–P(4)	99.3(1)	P(3)–Re–P(4)	77.9(1)
P(1)–Re–Cl(1)	77.8(1)	P(2)–Re–Cl(1)	80.9(1)
P(3)–Re–Cl(1)	89.7(1)	P(4)–Re–Cl(1)	87.1(1)
P(1)–Re–C(61)	97.9(2)	P(2)–Re–C(61)	94.9(2)
P(3)–Re–C(61)	94.6(2)	P(4)–Re–C(61)	97.3(2)
Cl(1)–Re–C(61)	174.4(2)	Re–C(61)–C(62)	175.2(5)

Table 3 Selected bond distances (Å) and angles (°) for complex **3**

Re–O(1w)	2.250(6)	Re–Cl(1)	2.408(2)
Re–P(1)	2.521(2)	Re–P(2)	2.484(2)
Re–C(37)	1.784(8)	Re–C(47)	1.970(6)
C(37)–C(38)	1.424(11)		
O(1w)–Re–Cl(1)	81.8(1)	O(1w)–Re–P(1)	87.7(2)
Cl(1)–Re–P(1)	92.5(1)	O(1w)–Re–P(2)	87.2(2)
Cl(1)–Re–P(2)	83.2(1)	P(1)–Re–P(2)	173.7(1)
O(1w)–Re–C(37)	174.9(2)	Cl(1)–Re–C(37)	103.3(2)
P(1)–Re–C(37)	92.6(2)	P(2)–Re–C(37)	92.8(2)
O(1w)–Re–C(47)	86.4(3)	Cl(1)–Re–C(47)	168.2(2)
P(1)–Re–C(47)	86.3(2)	P(2)–Re–C(47)	97.0(2)
C(37)–Re–C(47)	88.5(3)	Re–C(37)–C(38)	179.4(5)

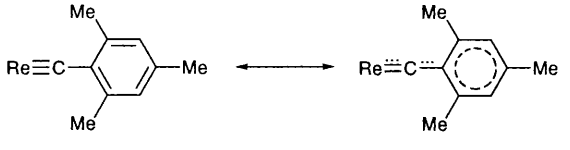

Complex **3** has a distorted-octahedral structure. The benzylidyne ligand is *trans* to a co-ordinated water with a C(37)–Re–O(1w) angle of 174.9(2)°. The extremely long Re–O(1w) distance of 2.250(6) Å is in accordance with the large *trans*-labilizing effect of the benzylidyne group. The Re–C(37) distance of 1.784(8) Å is slightly shorter than that in **2**, but, presumably, a π-electron delocalization still exists within the $Re{\equiv}CC_6H_2Me_3$ unit. The Re–C(37)–C(38) angle of 179.4(5)° is similar to the related 175.2(5)° in **2**. The two triphenylphosphine ligands are *trans* to each other with P(1)–Re–P(2) 173.7(1)°. The chloride group is *cis* to the benzylidyne ligand, and the Re–Cl distance of 2.408(2) Å is shorter than that in **2** in which the chloride is *trans* to the benzylidyne ligand.

Electronic absorption and emission spectra

The UV/VIS spectral data for the complexes are listed in Table 4. As a representative example, the absorption spectrum of **2** is shown in Fig. 3. In general, the complexes exhibit intense absorption bands at 318–330 nm and weak absorptions in the 405–470 nm region. The large absorption coefficients observed for the high-energy bands suggest their origins as charge-transfer transitions, presumably $Re^V \longrightarrow \pi^*$ ($Re{\equiv}CC_6H_2Me_3$) or $Re^V \longrightarrow$ (phosphine)*. With reference to previous spectroscopic works by Winkler and Gray[1b] on dioxorhenium(V) complexes and Mayr and co-workers[5a] on tungsten(IV)-alkylidyne complexes, the energies of the 5d orbitals of rhenium(V)–alkylidyne complexes are likely to be in the order: $d_{xy} < d_{\pi^*}(d_{xz},d_{yz}) < d_{x^2-y^2} < d_{z^2}$. The low-energy absorptions probably arise from a $d_{xy} \longrightarrow d_{\pi^*}$ (d_{xz},d_{yz}) transition. Changing the solvent from dichloromethane to acetonitrile has little effect on the UV/VIS spectra.

Excitation of the complexes in solution, solid or glassy states at 300–450 nm gives intense orange to red emissions. The photophysical data are summarized in Table 5. The large difference in emission and lowest-allowed absorption energies and the long emission lifetimes suggest that the transitions involved are due to spin-forbidden processes. The $^3[(d_{xy})^1(d_{\pi^*})^1]$ is most likely to be the emissive state.

The low-temperature emission spectra of the complexes are rich in vibrational fine structure. Fig. 4 shows the emission spectra of complexes **2** and **5** at 77 K. The vibrational progressions in the two cases average around 1050 cm^{-1} and are assigned to the $\nu(Re{\equiv}CC_6H_2Me_3)$ stretch in the $^3[(d_{xy})^1(d_{\pi^*})^1]$ excited states. Vibronic structured emission has previously been reported for the dioxorhenium(V) system.[1]

The auxiliary ligands do affect the photophysical data for the rhenium(V)–benzylidyne complexes. As shown in Table 5, changing the non-chromophoric ligands results in a systematic variation in E_{em}. The radiationless decay constants increase as the emission maxima shift to lower energies. Fig. 5 shows a plot of ln k_{nr} *vs.* the emission energy E_{em}. The observed linear correlation is consistent with the energy-gap law for radiationless transitions.[10] This predicts that, for a series of related excited states based on the same chromophore, the radiationless decay rate constants are largely determined by the vibrational overlap between the ground and excited states. Using the expression derived by Englman and Jortner,[10a] in the low-temperature and weak vibrational coupling limit k_{nr} is given approximately by equation (1). In this equation ΔE is the

$$k_{nr} = (2\pi V^2/\hbar)(\tfrac{1}{2}\pi\hbar\omega_M\Delta E)^{\frac{1}{2}} \exp(-S) \exp(-\gamma\Delta E/\hbar\omega_M) \quad (1)$$

Table 4 The UV/VIS spectra data for the complexes (R = $C_6H_2Me_3$-2,4,6) at room temperature

Complex	λ_{max}/nm	ε_{max}/dm^3 mol^{-1} cm^{-1}
2 [Re(CR)(pdpp)$_2$Cl]ClO$_4$	318	13 800
	410[a]	450
3 [Re(CR)(PPh$_3$)$_2$(CO)(H$_2$O)Cl]ClO$_4$	321	13 900
	420[a]	220
4 [Re(CR){P(C$_6$H$_4$OMe-*p*)$_3$}$_2$(CO)(H$_2$O)Cl][O$_3$SCF$_3$]	320	5 920
	430[b]	270
5 [Re(CR)(PMePh$_2$)$_2$(CO)(H$_2$O)Cl]ClO$_4$	320	12 100
	405[a]	470
6 [Re(CR)(dppe)(CO)$_2$Cl]ClO$_4$	330	7 290
	450[a]	200

[a] In dichloromethane. [b] In acetonitrile.

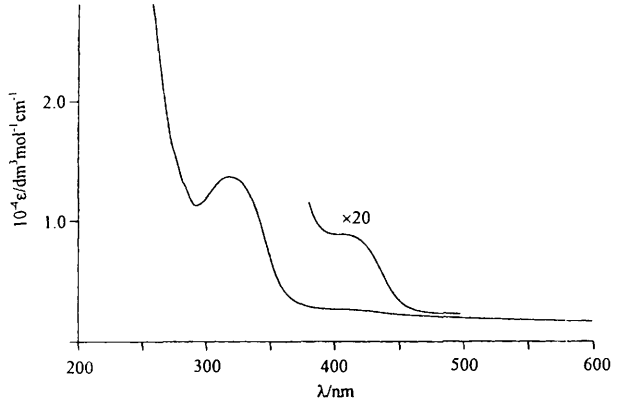

Fig. 3 The UV/VIS absorption spectrum of complex **2** in acetonitrile

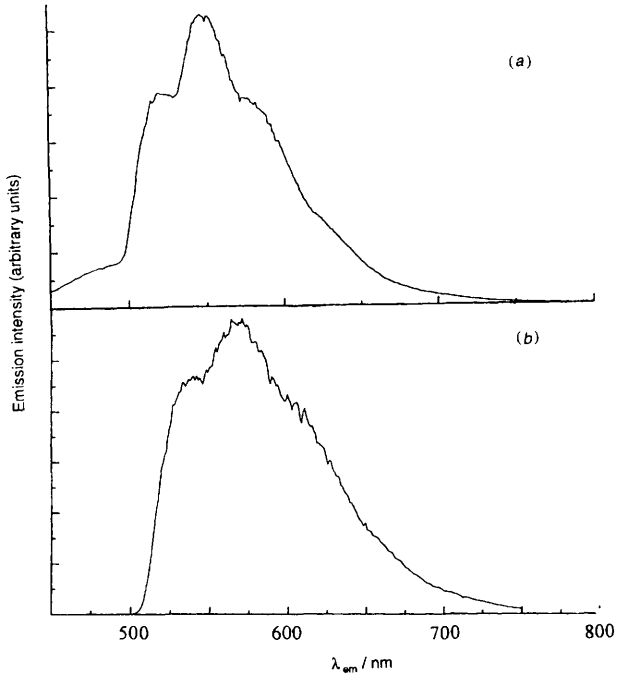

Fig. 4 Emission spectra at 77 K: (*a*) [Re(CC$_6$H$_2$Me$_3$-2,4,6)(pdpp)$_2$Cl]ClO$_4$, glassy state in *n*-butyronitrile, $\lambda_{excitation}$ = 320 nm; (*b*) [Re(CC$_6$H$_2$Me$_3$-2,4,6)(PMePh$_2$)$_2$(CO)(H$_2$O)Cl]ClO$_4$, solid state, $\lambda_{excitation}$ = 350 nm

internal energy gap between the upper and lower states, ω_M is the frequency of the deactivating mode or modes, V is the electron-tunnelling matrix element, γ and S are defined in equations (2) and (3) respectively and Δ_j is the dimensionless

$$\gamma = \ln(2\Delta E/\Sigma\hbar\omega_j\Delta_j^2) - 1 \quad (2)$$

Table 5 Excited-state decay parameters for the emission of the complexes in dichloromethane at room temperature

Complex	$10^{-3}E_{em}$/cm^{-1}	τ/μs	φ_{em}	k_r/s^{-1}	k_{nr}/s^{-1}
2	17.45	2.08	0.042	2.02×10^4	4.61×10^5
3	17.24	2.25	0.0020	8.89×10^2	4.43×10^5
4	17.01	1.76	0.0067	3.81×10^3	5.68×10^5
5	16.37	0.95	0.0046	4.84×10^3	1.05×10^6
6	17.64	3.35	0.0035	1.05×10^3	2.97×10^5

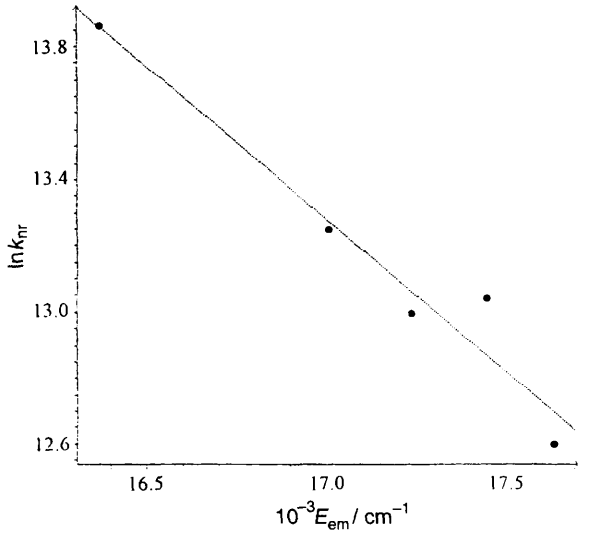

Fig. 5 Plot of ln k_{nr} *vs.* E_{em} for emission of the rhenium(V)–benzylidyne complexes in dichloromethane at room temperature

$$S = \tfrac{1}{2}\Sigma\Delta_j^2 \quad (3)$$

fractional displacement between the equilibrium nuclear configurations of the ground and excited states for the complex's *j*th normal mode. In comparing a series of related excited states, if the deactivating mode or modes remain common and variations in V and S are relatively small, as is the case for a series of polypyridyl complexes of osmium(II),[11] equation (1) can be simplified to (4) where ΔE is assumed to be

$$\ln k_{nr} = (\ln\beta - S) - (\gamma E_{em}/\hbar\omega_M) \quad (4)$$

E_{em}. If the assumptions are valid a linear relation should exist between ln k_{nr} and E_{em}. From the results shown in Fig. 5 there is a good agreement between theory and experiment. Thus the rhenium(V)–benzylidyne complexes are another good example of the application of the energy-gap law to the excited states of organometallic complexes.

Electrochemistry and excited-state reduction potentials

Complex **2** shows well defined electrochemical properties. In acetonitrile solution, reduction of the complex has not been observed even at a potential of −2.0 V *vs.* Ag–AgNO$_3$ (0.1 mol dm^{-3}). However it displays a reversible oxidation couple with $E_{\frac{1}{2}}$ at 1.15 ± 0.02 V. Constant-potential electrolysis at 1.2 V established n = 1.0 ± 0.1, suggesting that the electrode reaction is a one-electron oxidation process. This is tentatively assigned to the oxidation of Re^V to Re^{VI}. Should this be the case, this would mean the generation of a highly oxidizing rhenium(VI)–benzylidyne complex. However, the oxidized product was unstable on the time-scale of this experiment (≈30 min to 1 h). The excited-state reduction potential for reaction (5) was estimated using equation (6) where $E_{0\text{-}0}$ is the zero–zero

$$Re^{VI} + e \longrightarrow Re^{V*} \quad (5)$$

$$E^\circ(Re^{VI}\text{–}Re^{V*}) \approx E_{\frac{1}{2}}(Re^{VI}\text{–}Re^{V}) - E_{0\text{-}0}(Re^{V*}) \quad (6)$$

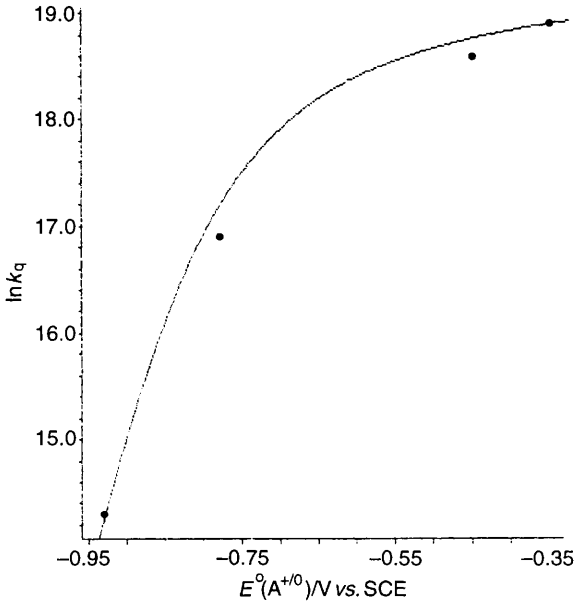

Fig. 6 Plot of ln k_q *vs.* $E^\circ(A^{+/0})$ for the oxidative quenching of complex **2** by pyridinium acceptors in degassed acetonitrile: (●) experimental data; (—) theoretical curve

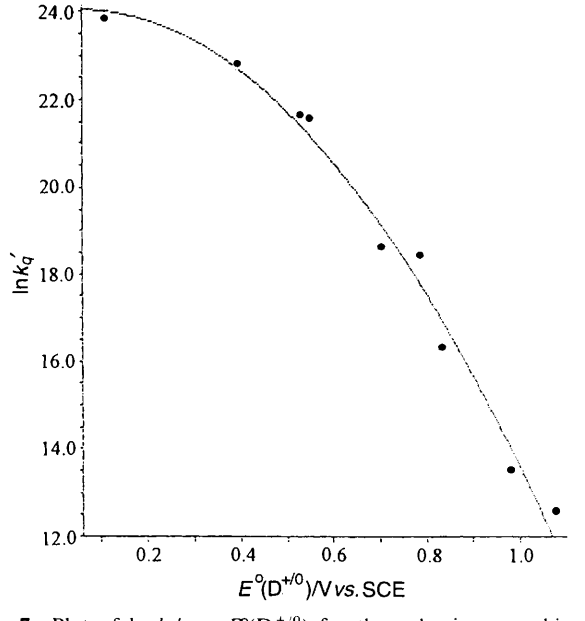

Fig. 7 Plot of ln k_q' *vs.* $E^\circ(D^{+/0})$ for the reductive quenching of complex **3** by amine donors in degassed acetonitrile; symbols as in Fig. 6

emission energy. From the low-temperature emission spectrum [Fig. 4(*a*)], $E_{0\text{-}0}(Re^{V}*)$ is estimated to be 520 nm (2.38 eV). Thus $E^\circ(Re^{VI}\text{–}Re^{V}*)$ is −1.23 V *vs.* Ag–$AgNO_3$, that is −0.90 V *vs.* SCE, suggesting that the $^3[(d_{xy})^1(d_{\pi^*})^1]$ state of complex **2** is a good one-electron reductant.

In contrast to complex **2**, the cyclic voltammogram of **6** in acetonitrile shows no oxidation couple even at potentials up to +2.0 V *vs.* Ag–$AgNO_3$ (0.1 mol dm^{-3}). This is not surprising since the co-ordinated CO in **6** should not favour oxidation of the metal complex. However, an irreversible reduction wave at an E_{pc} of −1.87 ± 0.02 V, tentatively assigned to the reduction of Re^{V} to Re^{IV}, was observed. Although the Re^{V}–Re^{IV} couple is irreversible, E_{pc} can be taken as the upper limit of $E_{\frac{1}{2}}(Re^{V}\text{–}Re^{IV})$. The excited-state redox potential for reaction (7) can be estimated using equation (8). The $E^\circ(Re^{V}*\text{–}Re^{IV})$ of **6** is,

$$Re^{V}* + e \longrightarrow Re^{IV} \quad (7)$$

$$E^\circ(Re^{V}*\text{–}Re^{IV}) \approx E_{\frac{1}{2}}(Re^{V}\text{–}Re^{IV}) + E_{0\text{-}0}(Re^{V}*) \quad (8)$$

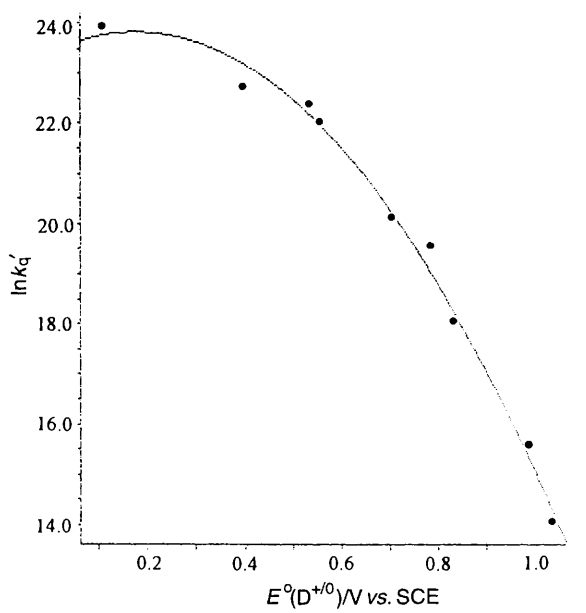

Fig. 8 Plot of ln k_q' *vs.* $E^\circ(D^{+/0})$ for the reductive quenching of complex **6** by amine donors in degassed acetonitrile; symbols as in Fig. 6

therefore, estimated to have an upper limit of 0.72 V *vs.* Ag–$AgNO_3$ or 1.05 V *vs.* SCE taking $E_{0\text{-}0}(Re^{V}*)$ to be 480 nm (2.59 eV) from the emission spectrum at 77 K.

Photoinduced electron-transfer reactions

Not surprisingly, the luminescence of complex **2** is quenched by pyridinium acceptors and the others having carbonyl ligands are quenched by amine donors. To understand further the electron-transfer reactivity of the $^3[(d_{xy})^1(d_{\pi^*})^1]$ excited states, a study of the luminescence quenching by a series of quenchers having different E° values was undertaken. The quenching rate constants were obtained from Stern–Volmer plots corrected for the diffusion-controlled rate constants. The results are summarized in Tables 6–8. The rate constants exhibit a dependence upon the reduction potentials of the pyridinium salts or the amine oxidation potentials. The values of $E^\circ(Re^{IV}\text{–}Re^{V}*)$ or $E^\circ(Re^{V}*\text{–}Re^{IV})$ were obtained by three-parameter, non-linear least-squares fits using equation (9),[15] where the

$$(RT/F)\ln k_q' = (RT/F)\ln K_{12}\kappa\nu_{23} - [\lambda(1 + \Delta G_{23}/\lambda)^2/4] \quad (9)$$

symbols refer to the reactions shown in Schemes 2 (for **2**) and 3 (for **3** and **6**), $K_{12} = k_{12}/k_{21}$, ν_{23} is the effective nuclear vibrational frequency, κ is the electronic transmission coefficient ($\kappa = 1$ for a bimolecular electron-transfer reaction) and λ is the total reorganization energy associated with the inner and outer co-ordination spheres. For oxidation quenching, ΔG_{23}, the standard free-energy change of the reaction, is given by equation (10), and for reduction

$$\Delta G_{23}/V = E^\circ(Re^{VI}\text{–}Re^{V}*) - E(A^{+/0}) + w_p - w_r \quad (10)$$

quenching, it is given by equation (11). In both equations w_p

$$\Delta G_{23}/V = -E^\circ(Re^{V}*\text{–}Re^{IV}) + E(D^{+/0}) + w_p - w_r \quad (11)$$

and w_r are the respective work terms for bringing the reactants and products to the mean separation for the reactions. For weak interactions the work terms are due to coulombic interactions and, therefore, are practically zero when at least one of the two reaction partners is neutral. Thus ΔG_{23} can simply be taken as in equation (12) for oxidation quenching and (13) for reduction quenching.

Table 6 Rate constants for the oxidative quenching of complex **2** by pyridinium salts in acetonitrile at room temperature

Quencher (A)*	$E°(A^+–A)$/V *vs.* SCE	k_q/dm^3 mol^{-1} s^{-1}	ln k_q
N,*N*′-Dibenzyl-4,4′-bipyridinium	−0.35	(1.56 ± 0.10) × 10^8	18.87 ± 0.06
N,*N*′-Dimethyl-4,4′-bipyridinium	−0.45	(1.24 ± 0.03) × 10^8	18.64 ± 0.02
4-Cyano-*N*-methylpyridinium	−0.67	(1.04 ± 0.02) × 10^8	18.46 ± 0.02
4-Methoxycarbonyl-*N*-methylpyridinium	−0.78	(2.14 ± 0.04) × 10^7	16.88 ± 0.02
4-Amido-*N*-ethylpyridinium	−0.93	(1.57 ± 0.10) × 10^6	14.3 ± 0.06

* All compounds are hexafluorophosphate salts.

Table 7 Rate constants for the reductive quenching of complex **3** by amine donors in acetonitrile at room temperature

Quencher (D)	$E°(D^+–D)$/V *vs.* SCE	k_q/dm^3 mol^{-1} s^{-1}	ln k_q' [a]
N,*N*,*N*′,*N*′-Tetramethyl-1,4-phenylenediamine	0.11 [b]	(1.06 ± 0.02) × 10^{10}	23.84 ± 0.04
1,4-Phenylenediamine	0.39	(5.73 ± 0.14) × 10^9	22.81 ± 0.03
Phenothiazine	0.53 [b]	(2.27 ± 0.10) × 10^9	21.66 ± 0.05
Benzidine	0.55 [c]	(2.13 ± 0.03) × 10^9	21.59 ± 0.02
Diethylaniline	0.70 [c]	(1.21 ± 0.07) × 10^8	18.62 ± 0.05
Dimethylaniline	0.78 [d]	(1.05 ± 0.02) × 10^8	18.47 ± 0.02
Diphenylamine	0.83 [d]	(1.21 ± 0.03) × 10^7	16.30 ± 0.03
Aniline	0.98 [d]	(7.31 ± 0.37) × 10^5	13.50 ± 0.05
p-Chloroaniline	1.07 [b]	(2.88 ± 0.03) × 10^5	12.57 ± 0.01

[a] $1/k_q' = (1/k_q) - (1/k_{diff})$ where $k_{diff} = 2 \times 10^{10}$ dm^3 mol^{-1} s^{-1}. [b] Ref. 14. [c] Ref. 13. [d] Ref. 12.

Table 8 Rate constants for the reductive quenching of complex **6** by amine quenchers in acetonitrile at room temperature

Quencher (D)	$E°(D^+–D)$/V *vs.* SCE	k_q/dm^3 mol^{-1} s^{-1}	ln k_q'
N,*N*,*N*′,*N*′-Tetramethyl-1,4-phenylenediamine	0.11	(1.10 ± 0.04) × 10^{10}	23.92 ± 0.08
1,4-Phenylenediamine	0.39	(5.38 ± 0.09) × 10^9	22.72 ± 0.02
Phenothiazine	0.53	(4.17 ± 0.12) × 10^9	22.39 ± 0.03
Benzidine	0.55	(3.12 ± 0.12) × 10^9	22.03 ± 0.05
Diethylaniline	0.70	(5.60 ± 0.18) × 10^8	20.17 ± 0.03
Dimethylaniline	0.78	(3.18 ± 0.12) × 10^8	19.59 ± 0.04
Diphenylamine	0.83	(6.97 ± 0.06) × 10^7	18.06 ± 0.01
Aniline	0.98	(5.87 ± 0.24) × 10^6	15.59 ± 0.03
Hydroquinone	1.03	(1.34 ± 0.10) × 10^6	14.11 ± 0.07

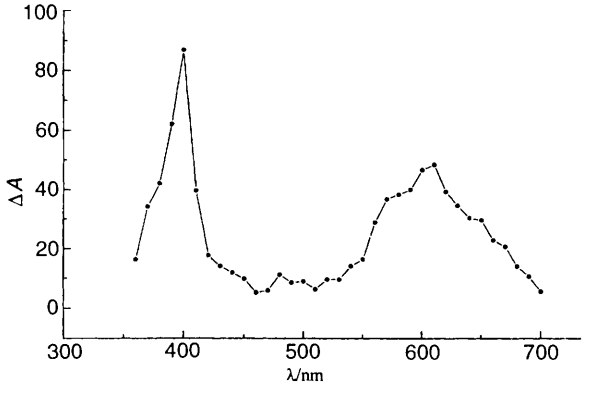

Fig. 9 Transient difference absorption spectrum recorded 20 μs after 355 nm excitation of a degassed acetonitrile solution of complex **2** (10^{-4} mol dm^{-3}) and *N*,*N*′-dimethyl-4,4′-bipyridinium hexafluorophosphate (10^{-3} mol dm^{-3}) at room temperature

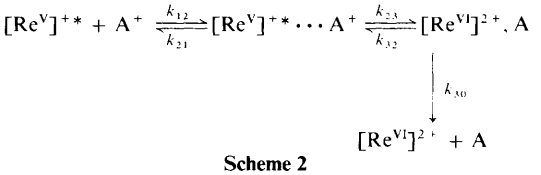

Scheme 2

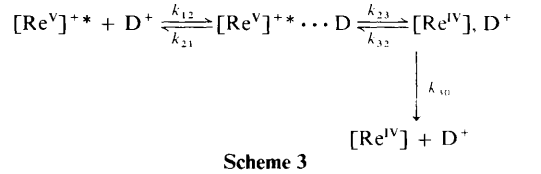

Scheme 3

$$\Delta G_{23}/V = E°(Re^{VI}–Re^{V}*) - E(A^{+/0}) \quad (12)$$

$$\Delta G_{23}/V = -E°(Re^{V}*–Re^{IV}) + E(D^{+/0}) \quad (13)$$

Figs. 6–8 show the theoretical curves obtained upon fitting of the data by equation (9). The value of $E°(Re^{VI}–Re^{V}*)$ for complex **2** is −0.85(5) V *vs.* SCE and $E°(Re^{V}*–Re^{IV})$ is +0.89(6) for **3** and +0.88(2) V for **6**. The results obtained from Stern–Volmer quenching experiments agree well with our estimation from spectroscopic and electrochemical data. The excellent agreement of the experimental data with those predicted from Marcus theory suggests that electron transfer is the predominant luminescence quenching mechanism of the excited states. This is further supported by the results of flash-photolysis experiments. Upon flashing a degassed acetonitrile solution of **2** and *N*,*N*′-dimethyl-4,4′-bipyridinium hexafluorophosphate the relatively long-lived *N*,*N*′-dimethyl-4,4′-bipyridinium radical with λ_{max} at 400 and 610 nm was produced (Fig. 9). Similarly, flashing a degassed acetonitrile solution of **3** and *N*,*N*,*N*′,*N*′-tetramethyl-1,4-phenylenediamine gave the *N*,*N*,*N*′,*N*′-tetramethyl-1,4-phenylenediamine radical cation,

which shows an intense broad absorption band ranging from 525 to 600 nm.[16]

It is not surprising that co-ordinated CO affects the redox properties of the excited states. The two strong σ-donor ligands pdpp would make the Re^{V} more electron rich, so the excited state of complex **2** is strongly reducing. On the contrary, the π-acceptor level of the co-ordinated CO makes the excited state of **3**–**6** easily reduced and accounts for their oxidizing properties.

Conclusion

The present work highlights that rhenium(V)–benzylidyne complexes are of interest in organometallic photochemistry. These complexes should be easily accessible and their excited-state properties easily tuned by ligand modifications. Given the antibonding nature of the d_{π^*} orbital, the $Re{\equiv}CC_6H_2Me_3$ bond is likely to be weakened in the $^3[(d_{xy})^1(d_{\pi^*})^1]$ excited state. Thus it would not be surprising to find these complexes undergo photoinduced $CC_6H_2Me_3$ group-transfer reactions.

Acknowledgements

We acknowledge support from The University of Hong Kong, the Croucher Foundation and the Hong Kong Research Grants Council.

References

1 J. R. Winkler and H. B. Gray, (*a*) *J. Am. Chem. Soc.*, 1983, **105**, 1373; (*b*) *Inorg. Chem.*, 1985, **24**, 346.

2 C. M. Che, T. C. Lau, H. W. Lam and C. K. Poon, *J. Chem. Soc., Chem. Commun.*, 1989, 114; C. M. Che, M. H. W. Lam and T. C. W. Mak, *J. Chem. Soc., Chem. Commun.*, 1989, 1529; H. W. Lam, C. M. Che and K. Y. Wong, *J. Chem. Soc., Dalton Trans.*, 1992, 1411; C. M. Che, K. Y. Wong, H. W. Lam, K. F. Chin, Z. Y. Zhou and T. C. W. Mak, *J. Chem. Soc., Dalton Trans.*, 1993, 857; K. F. Chin, K. K. Cheung, H. K. Yip, T. C. W. Mak and C. M. Che, *J. Chem. Soc., Dalton Trans.*, 1995, 657.

3 V. W. W. Yam, C. M. Che and W. T. Tang, *J. Chem. Soc., Chem. Commun.*, 1988, 100; V. W. W. Yam and C. M. Che, *Coord. Chem. Rev.*, 1990, **97**, 93; K. F. Chin, K. K. Cheung, C. X. Guo and C. M. Che, *J. Chem. Soc., Dalton Trans.*, 1995, 2967.

4 G. A. Neyhart, M. Bakir, J. Boaz, W. J. Vining and B. P. Sullivan, *Coord. Chem. Rev.*, 1991, **111**, 27.

5 (*a*) A. B. Bocarsly, R. E. Cameron, H. D. Rubin, G. A. McDermott, C. R. Wolff and A. Mayr, *Inorg. Chem.*, 1985, **24**, 3976; (*b*) J. D. Carter, K. B. Kingsbury, A. Wilde, T. K. Schoch, C. J. Leep, E. K. Pham and L. McElwee-White, *J. Am. Chem. Soc.*, 1991, **113**, 2947.

6 (*a*) A. J. L. Pombeiro, M. F. N. N. Carvalho, P. B. Hitchcock and R. L. Richards, *J. Chem. Soc., Dalton Trans.*, 1981, 1629; (*b*) A. J. L. Pombeiro, A. Hills, D. L. Hughes and R. L. Richards, *J. Organomet. Chem.*, 1988, **352**, C5; (*c*) J. K. Felixberger, P. Kiprof, E. Herdtweck, W. A. Herrmann, R. Jakobi and P. Gütlich, *Angew. Chem., Int. Ed. Engl.*, 1989, **28**, 334; (*d*) D. S. Williams and R. R. Schrock, *Organometallics*, 1994, **13**, 2101.

7 D. D. Perrin and W. L. F. Armarego, *Purification of Laboratory Chemicals*, 2nd edn., Pergamon, Oxford, 1980.

8 G. M. Sheldrick, *Computational Crystallography*, ed. D. Sayre, Oxford University Press, New York, 1992, pp. 506–514; *SHELXTL-PC User Manual*, Siemens Analytical Instruments, Madison, WI, 1990.

9 J. N. Demas and G. A. Crosby, *J. Phys. Chem.*, 1971, **75**, 991.

10 (*a*) R. Englman and J. Jortner, *Mol. Phys.*, 1970, **18**, 145; (*b*) K. F. Freed and J. Jortner, *J. Chem. Phys.*, 1970, **52**, 6272.

11 J. V. Caspar, E. M. Kober, B. P. Sullivan and T. J. Meyer, *J. Am. Chem. Soc.*, 1982, **104**, 630; J. V. Caspar and T. J. Meyer, *J. Phys. Chem.*, 1983, **87**, 952.

12 M. A. Fox and M. Chanon, *Photoinduced Electron Transfer*, Elsevier, New York, 1988, Part D.

13 C. W. Chan, Ph.D. Thesis, University of Hong Kong, 1994.

14 C. K. Mann and K. K. Barnes, *Electrochemical Reaction in Non-aqueous Systems*, Marcel Dekker, New York, 1970.

15 C. R. Bock, J. A. Connor, A. R. Gutierrez, T. J. Meyer, D. G. Whitten, B. P. Sullivan and J. K. Nagle, *J. Am. Chem. Soc.*, 1979, **101**, 4815.

16 K. Kawai, N. Yamamoto and H. Tsubomura, *Bull. Chem. Soc. Jpn.*, 1969, **42**, 369.

Received 23*rd January* 1996; *Paper* 6/00514D